MUST Journal of Research and Development (MJRD) Volume 5 Issue 3, September 2024
e ISSN 2683-6467 & p ISSN 2683-6475

Determining Bandgap of Thermochromic Phosphor Films via Reflectance Measurements under Controlled Heating

Steven Rwabona Katashaya

Kabale University

P.O. Box 317, Kabale, Uganda

DOI: https://doi.org/10.62277/mjrd2024v5i30054

ARTICLE INFORMATION

Article History

Received: 16th April 2024
Revised: 16th May 2024
Accepted: 24th May 2024
Published: 02nd September 2024

Keywords
Reflectance
Absorbance
Thermochromism
Phosphors
Bandgap
Activation energy

ABSTRACT

In this article, we present a method to determine the bandgap of a thermochromic phosphor film by simple reflectance measurements under controlled heating. The phosphor is illuminated by a light-emitting diode while being heated continuously. The reflected light is detected using a calibrated photodiode circuit based on an operational transconductance amplifier. We apply the Schuster-Kubelka-Munk function to deduce the absorbance over temperature and thus the bandgap. We show, for the first time, that the thermochromic phosphor's colour change follows Arrhenius's Law and therefore involves activation energy. We estimate the bandgap to be between 1.1 eV and 1.9 eV and find an activation energy of 46.67 ±1.6 kJ/mol. The simplicity of the approach will appeal to undergraduate teachers and students of physics and materials science. The technique can be used to investigate other thermochromic materials as well.

*Corresponding author's e-mail address: srkatashaya@kab.ac.ug (Katashaya S.R.)

1.0 Introduction

Reflectance is a phenomenon in which the surface of a material reflects some of the radiation that is directed onto it. The extent of this reflection depends on several factors, such as the spectral composition of the incident radiation and the surface texture. The latter dictates whether the reflection is specular (smooth) or diffuse. The material's refractive index and absorption coefficient are combined to quantify the reflectance in terms of a single index called reflectivity (Kortum 2012). The highly successful Kubelka-Munk theory (Kubelka 1948, Kubelka 1954) and its refinements (Zanatta 2019, Myrick et al. 2011) encapsulate the basic idea behind reflectance spectroscopy. Reflectance spectroscopy is an important, well-established technique in almost all areas of the physical sciences. For instance, it has proved invaluable in determining optical bandgap in semiconductors (Pankove 1975), in in vivo kinetic studies of biological systems for their non-invasive nature (Hoffmam et al., 1998; Ala-Laurila et al., 2004), and in establishing chemical dynamics (Weckhuysen et al., 2000). The ubiquity of electronic and solid-state devices is mostly due to the ability to do optical measurements, particularly absorption on materials. The optical properties of a material are the sum of its interactions with the incident electromagnetic field. These wave-like, quantum-mechanically modelled properties are intrinsically linked and inseparable from the material's electronic band structures and atomic energy levels. The determination of these properties through classically defined photon energy is, therefore, of fundamental importance to the study of the material. The classification of material as either direct or indirect bandgap depends on how an electron traverses the forbidden energy gap or bandgap. Transitions in indirect bandgap materials involve at least one photon and one phonon quantum.

The current flurry of research into new semiconductors has demonstrated significant variability and frequent misuse of models for absorption coefficients from reflectance and transmittance measurements. Several model estimates of the fundamental absorption coefficient are currently in use for semiconductors. However, the success of a model depends on the structure of the material. In a recent review, Zanatta (2019) demonstrates that often, researchers have incorrectly and indiscriminately applied models such as Tauc's method (Tauc 1968) to ordered, crystalline semiconductors that are more useful for amorphous semiconductors where diffuse reflections happen. Zanatta (2019) also proposes a unified model to fit the absorption coefficient to a sigmoid Boltzmann function (Davis and Mott 1971; Li et al. 2013; Dolgonos et al. 2016).

In this article, we attempt to answer the question of the impact of both photons and phonons on the electron transitions of a reversible thermochromatic paint. Although the mechanism of thermochromism has been known for several decades, it is now receiving increased attention due to its apparent ability to tune the bandgap of hybrid semiconductors (Day and Joachim 1965, Li et al. 2013, Zhang et al. 2017). The full mechanisms of thermochronism are not fully understood. In metal-halide perovskites, for instance, it is believed that it arises from the modification of the distances between the halide atom (e.g., Cl) and the metal (e.g., Pb) (Zhang et al. 2017). We devise a simple experimental setup that involves measuring the reflected light from a film while subjecting it to a controlled source of heat at a discrete wavelength. The reflected light is detected using a calibrated photodiode (PD) conditioned by an operational transconductance amplifier (TCA) circuit. The experiment is repeated for a number of wavelengths chosen to be within the extremes of the visible spectrum. In this experiment, we first determine the phosphor reflectivity behaviour at specified wavelengths over a known temperature range. Then, we deduce the absorbance as a function of wavelength by using the data obtained in the previous step. Thermochromic pigments are amorphous or nanoparticle-based. We apply the Schuster-Kubelka-Munk (SKM) relation to analyse the behaviours of a commonly used thermochromic pigment. The SKM is reportedly suitable for such diffusely reflecting samples (Kubelka 1954, Schuster 1905). After determining the reflectance and absorbance characteristics of the phosphor, we show that the colour change in the phosphor is specific to a temperature. This suggests that an activation energy mechanism is at play, i.e., energy is required to transform the structure of the active molecule into one that changes its colour reversibly. This energy is supplied by phonons. We show for the first time that Arrhenius's law is also applicable to the activation of the thermochromic phosphor. Laidler (1972) refers to several reported examples in nature where Arrhenius's law is applicable. In these examples, Arrhenius's law is

applied pedagogically as a tool to quantify event rates as functions of air temperature, such as the chirping of crickets, the movement of ants, the flashing of fireflies, and many other phenomena. More recently, Byrd and Perona (2005) followed a similar approach to describe the popping of corn in terms of the first-order kinetics that lead up to Arrhenius law. In short, taking this approach to explain complex concepts through intuitive examples can be appealing to new students.

2.0 Materials and Methods

2.1 Ethics Statement

This research did not involve human, biological or environmental entities.

2.2 Theory

In the semi-classical approach, the absorption coefficient is a consequence of the electron wave-vector selection rule:

$$\bar{k}_f = \bar{k}_i + \bar{k}_p \qquad (1)$$

Where $\bar{k}_i$ and $\bar{k}_f$ are, respectively, the initial and final electron momenta. The term $\bar{k}_p$ denotes any phonon momentum contribution. It accounts for any accompanying kinetic energy gain by the electron. If zero, then the transition is direct but otherwise, indirect. The selection rule is applied assuming no coulomb and magnetic forces at play and no impurities (Kortum 2012, Soref and Bennet 1987, Zwerdling et al.1957). Fig. 1 shows the scheme from which the absorption coefficient, α, is derived (Pankove 1975).

Figure 1
The Absorption Coefficient Schema Using Incident Intensity, I_0. The Coefficients of Reflection (R) and Transmission (T) are without I_0, and Lie between 0 and 1.

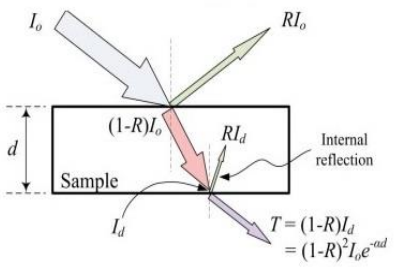

Hence, for a sufficiently large sample thickness, *d,* and no multiple internal reflections,

$$\alpha = \frac{1}{d} ln\left[\frac{(1-R)^2}{T}\right] \qquad (2)$$

An electron traverses the forbidden gap when it absorbs an amount of energy, *E,* that is greater than the bandgap. Thus,

$$\alpha \propto \left(E \pm E_p - E_g\right)^n \qquad (3)$$

where *n* = 1/2 and 2 for direct and indirect bandgap materials, respectively. The term $E_p = \hbar\omega$ describes, in terms of the phonon angular frequency ω,the phonon energy contribution to the final electron energy in indirect bandgap semiconductors. A negative E_p means that energy is also absorbed through a mechanical (phonon) process, such as the heating of the material. For most semiconductors, the contribution of E_p is small and can be ignored. Equation 3 assumes that impurity states - with energy levels normally located in the forbidden energy band - are not present. One can then write a form of Tauc's plot (Tauc 1968) for a phonon absorbing sample, i.e.

$$(\alpha h\nu)^{1/n} \propto \left(E - E_\beta\right) \qquad (4)$$

where the incident photon energy is $E_p = h\nu$ and $E_\beta = (E_p + E_g)$. Thus, a plot of $(\alpha h\nu)^{1/n}$ (i.e. the y-axis) versus E (the x-axis), when extrapolated to y=0, marks the onset energy for the optical transitions. This is equivalent to stating that $E = E_g$. Despite its successes, the Tauc plot does not provide any insight into whether the semiconductor itself is direct or indirect bandgap. For a thermochromic pigment, which directly responds to heat, the impact of phonons on the electron transitions cannot be ignored. The SKM approximation, based on apparent absorption, is applicable for samples that scatter diffusely (Zanatta 2019, Wendlandt and Hecht 1969), i.e.

$$\alpha \sim \frac{(1-R_\infty)^2}{2R_\infty} \qquad (5)$$

where R_∞ is the diffuse reflectance calibrated to a perfectly reflecting (i.e. non-absorbing) *standard,* defining the reference reflection at a given wavelength.

2.3 Reflection Standard

High accuracy reflection measurements use a large integrating (hemi)sphere to detect all the possible reflections. In this article, the source beam is directed towards the sample from a given distance and the reflection is monitored on a PD transconductance amplifier (TCA) shown in Fig. 2. The PD is from RS (pin-spot2d, 2019).

Figure 2

Circuit Diagram of the LED Driver and the Transconductance Amplifier Used in the Experiment

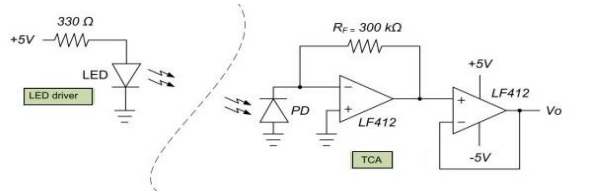

The sample illumination, heating and detection principle is shown in Fig. 3.

The PD is placed at a distance d_{pd} which is then maintained for all the light-emitting diode (LED) sources employed. Four LEDs were used. For each LED wavelength λ, the output of the TCA is recorded as the output of the TCA is recorded as $I^{\lambda}_{o,ref}$. This approach makes it unnecessary to know the precise incident intensity of the different LEDs. Since the same driver circuit is used for the different LEDs, there is variability in their intensities. A polished metallic surface comprising a computer disk drive platter was used as the standard. An estimate of R_{∞} using Equation 5 can then be obtained for the present case. The coefficient of reflection can then be calculated from the TCA output $I_{o,s}$ with a sample

$$R_{\infty}(\lambda) = I_{o,s}/I^{\lambda}_{o,ref} \qquad (6)$$

The voltage output of the TCA, V_o is directly proportional to the incident intensity. Therefore, all the intensities can be expressed as voltages. This experiment requires knowledge of the LED wavelengths. which can be obtained from the LED datasheet. Table 1 presents the results of the measurements on the LEDs. The reflection of the IR illumination from the polished standard was observed to be strongest.

Table 1
Measured Characteristics of the LEDs Used

LED Colour	Wavelength, λ (nm)	$I_{o,ref}$ (V)
Blue	452.9	0.035
Green	546.3	0.075
Red	671.1	0.036
Infra-red	925.8	2.438

The LEDs are placed close enough to the sample to illuminate a small spot, as shown in Fig. 3.

Figure 3

The Sample Illumination, Heating and Detection Principle

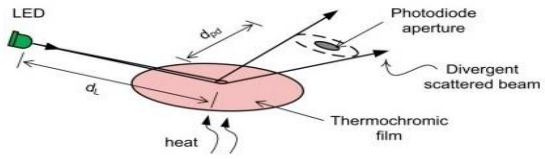

If the emission angle of the LEDs is ϑ, then it can be shown that the size of the approximately circular illuminated spot on the sample has an approximate radius $x \sim d_L \tan\vartheta$. The LEDs used have $\vartheta \sim 15^o$C and are placed at $d_L \approx 1$ cm. Hence $x \approx 2.6$ mm. For small d_{pd}, the solid angle formed by the reflected beam is small enough to fall consistently on the detection aperture of the PD. Therefore, the detection losses due to divergence of the reflected beams, which escape the detection aperture, are small. This makes it unnecessary in this experiment to have a large integrating sphere. The LED source and PD detector are mounted in close proximity in a compact, movable aluminium block. They are inset in the block such that the LED illumination does not fall on the PD without reflection. The relative alignment of LED and PD should be such that V_o is maximum when the standard approximately 1 cm away from the block.

The maximum in our case was about 1V for the blue LED and 3V for IR. Fig. 4 shows the positioning of the components.

Figure 4

Schematic Diagram Showing the Arrangement of the Measurement Components

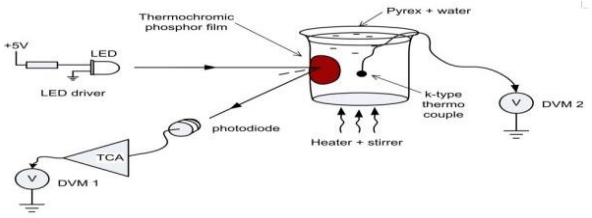

The digital multimeter labeled DVM2 has a temperature setting that allows readings in °C/F when connected to a Chromel-Alumel (k-type) thermo-couple.

2.4 Experimental

Fig. 5 shows the thermochromic phosphor used in this experiment. It is 'Black' when cold and 'Red' when Hot. The ilumination is made to fall a red-hot zone.

Figure 5

Photograph of the Food-box Label Thermochromic Film Used

The phosphor has an adhesive backing that allows it to be used as peel-off, temperature-sensitive food-box label. However, it can only indicate `hot' when red, and `cold' when black. Fig. 6 is a photograph of the polished metal platter used as the reflection standard. The image on the left appears dark because the standard has negligible diffuse reflection.

Figure 6

Two Photographs Showing the Reflection Standard

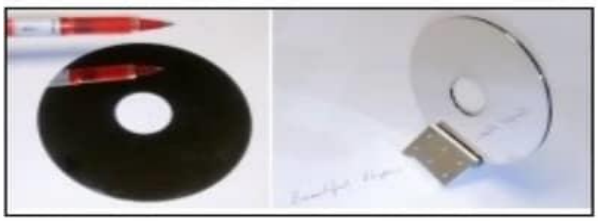

The experiment is done in a darkened room. The experimental procedure is as follows:

(a) Use Fig. 4 to position the apparatus.

(b) Place the standard in position for maximum TCA output. Record the distance, d_{pd}, from the block to the standard. Record V_o for each LED.

(c) Position the water-filled pyrex, which has the thermochromic label stuck on it, such that the phosphor is at the same distance and position in step (b) above.

(d) With the DVMs on, turn the heater on, with gentle stirring.

(e) Record T and V_o continuously as the pyrex heats up from room temperature to about 90 °C. Tabulate the results.

The previous step can be automated if a digital acquisition (DAQ) system is available. Alternatively, one can place the DVMs side-by-side and record a video of their displays on a mobile device as the experiment progresses. This provides a more leisurely transcribing of results by controlled playback by pausing/rewinding. However, video recording requires sufficient lighting. Therefore, the DVMs can be placed in additional lighting away from the PD. Ideally, DVMs with a back-lit mode can be used.

3.0 Results and Discussion

Fig. 7 and 8 show, respectively, the results of the measured reflectance and calculated absorbance based on the setup in Fig. 4.

Figure 7

Temperature Variation of Reference

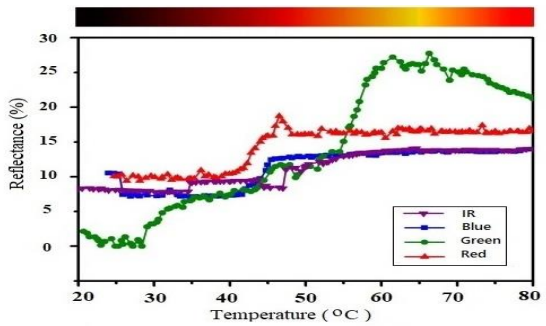

Figure 8

Temperature Variation of Adsorbance Calculated Using the Schuster-Kubelka-Munk Function (SKM)

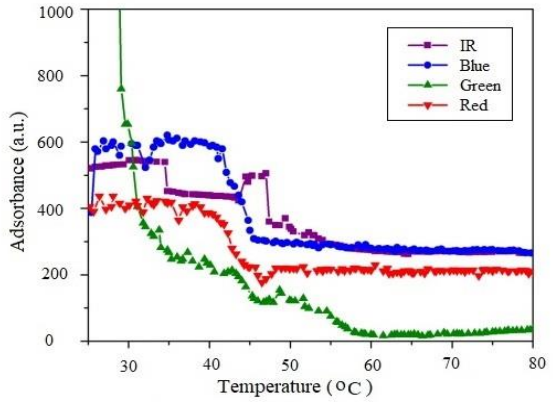

The plots show that the reflectance and absorbance of the thermochromic phosphor depend strongly on temperature. Both results show a strong response to the green wavelength. Below 30, the green reflectance is significantly lower than for all the other wavelengths. Over the entire experimental temperature range of 20 to 80 °C, all wavelengths except green are reflected almost equally. However, there is a marked increase in reflectance of all the colours between 40 and 50 The colour distribution spectrum in Fig. 7 was calculated using an online tool (RGB Colour Codes) from the plot data using the red-green-blue (RGB) reflectance values at the temperature. This calculation is based on light and colour standards maintained by the Commission Internationale de l'Eclairage (CIE). This standard combines lighting conditions with RGB color ratios to represent the color equivalent that the human eye actually sees.

Over the experimental temperature range, the red reflectance is consistently slightly higher than blue and green. Above 55, the reflectance of green increases significantly and dominates. It peaks around 60 and then gradually decreases beyond 80. Fig. 8 shows strong absorption of green below around 30. Visually, during the experiment, the thermochromic phosphor label used started to show its characteristic black-to-red colour change around 35 and remains a steady red colour beyond 60 This matches calculated CIE chromaticity. Intuitively, the strong green/red reflections simultaneously appear yellowish. These observations imply that the measurements capture the wavelength-sensitive reflections with excellent accuracy.

The accuracy of the intensity measurements can be improved by focussing the LEDs onto the sample using a convex lens with a short focal length. However, the intense spot should not inadvertently heat up the sample. Furthermore, we have assumed that the PD does not heat up during the experiment due to its proximity to the heat source. The reverse current through a PD, as with all semiconductor diodes, is highly sensitive to temperature. We took the precaution to minimise temperature sensitivity by mounting the PD in a small aluminium block, thereby implementing an isothermal block. Another assumption is that the thermochromic phosphor does not spontaneously emit photons by thermoluminescence (Bos 2017) as it heats up and changes colour. Such a mechanism would reinforce the detected beam and produce an incorrect result.

3.1 Estimates of the Bandgap

Singh and Ravindra (2010) describe the absorption spectra of some phthalocyanine- and porphyrin-based thermochromic materials as exhibiting two types of electronic transitions. These are the Soret or B-bands, as well as the Q-bands. These bands, if they exist in a material, will show up in the Tauc plot as two regions that extrapolate to two distinct bandgaps, and, respectively (Hamam 2017). Table 2 shows the bandgaps estimated using the sigmoid-Boltzmann function (Davis and Mott 1971) and the B-spline extrapolation of the data points.

Table 2
Measured Bandgaps, E_{gl} and E_{gh}

Temperature (°C)	E_{gl} (eV)	E_{gh} (eV)
30	-	1.95
40	1.20	2.07
50	0.68	1.63
80	1.14	1.96
$E_g \pm \Delta E_g$ (eV)	1.01±0.23	1.90±0.16
$\lambda \pm \Delta\lambda$ (nm)	1232±284	652±56

The bandgaps E_{gl} and E_{gh} shown in Table 2 are shown using arrows in Fig. 9 for 30°C, Fig. 10 for 40°C, Fig. 11 for 50°C and Fig. 12 for 80°C.

Figure 9
Tauc Plot, 30 ^{O}C

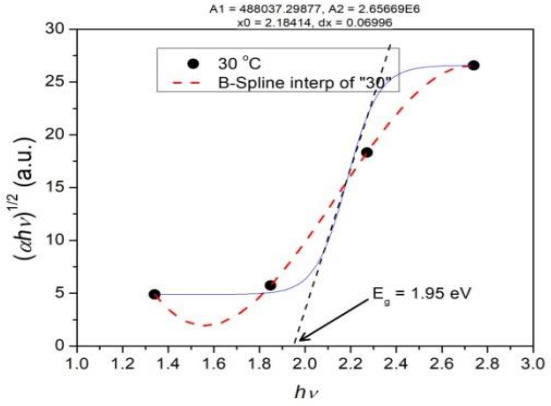

Figure 10
Tauc Plot, 40 ^{O}C

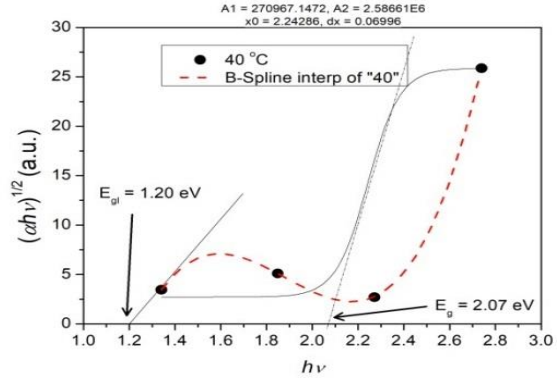

Figure 11
Tauc Plot, 50 ^{O}C

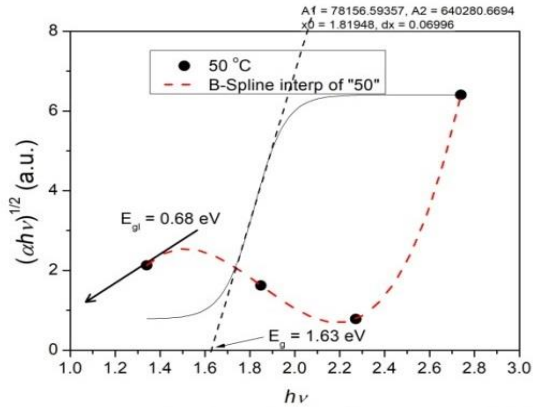

Figure 12
Tauc Plot, 80 ^{O}C

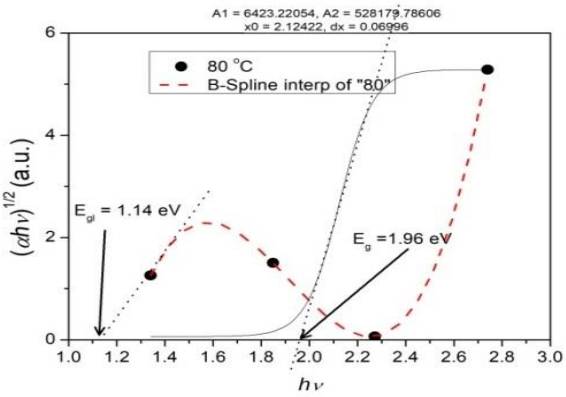

The presence of two or more bandgaps can be explained in terms of additional vibrational states in the material (Machado et al. 2011). The wavelengths in Table 2 start from the red part of the spectrum and extend into the infrared (595.8 - 1516.8) nm, shown in Fig. 13.

Figure 13
Spectrum Showing the Colour Associated with E_{gh} = 652 nm

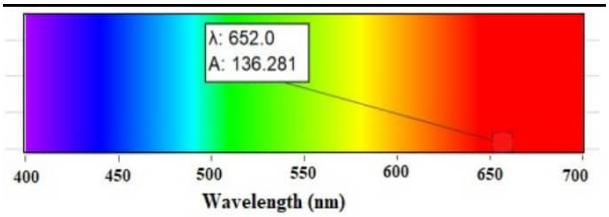

Several literatures have reported the bandgaps of lead-free perovskites in the range 1.5 - 2.5 eV (Zhang et al. 2017). As mentioned above, it is only recently that thermochromic materials have begun to receive considerable attention for their apparent ability to tune the bandgaps of other materials. The absorption calculated through the SKM function and plotted in Fig. 8 shows that the phosphor requires phonons to change its room-temperature reflectivity and absorbance. That is, it needs to be heated from 40 to 45 °C to start off a significant colour change.

3.2 Activation Temperature

A survey of current body of literature shows that not much research has been done to ascertain the activation energy of thermochromic materials. The most common encounter with thermochromic

materials is as dyes or pigments. Our foregoing discussions show, through reflectance in particular, that the phosphor's colour starts under a specific temperature relative to the ambient. This suggests that an activation energy mechanism is required. Although there are some mentions of activation temperature e.g. Fu and Hu (2017) and Salom et al. (2016), to the best of our knowledge an activation energy, has hitherto, neither been suggested nor calculated for these materials. Arrhenius's law (Laidler 1972) is expressed by the equation:

$$k = Ae^{-E_g/RT} \quad (7)$$

in terms of some activation energy, E_a. The term (RT) represents a molar kinetic energy at absolute temperature T, and R =8.314 J/K mol. If the heat-dependent process being modelled, such as the reflectance, can be expressed in terms of this law, then E_a exists. Equation 7 can be linearised, i.e.

$$\ln k = (-E_a)\frac{1}{RT} + \ln A. \quad (8)$$

Therefore, a plot of $y = ln\, k$versus $x = 1/(RT)$ should give a straight line with a negative gradient if an activation energy is involved. Fig. 14 plots Equation 8 for reflectance.

We find that E_a = 46.67 ± 1.62 kJ/mol and A = $e^{19.94}$ ~2.77 × 10^8. The high Pearson's coefficient of linearity of R^2 =0.932 implies a high-degree of plot linearity. This suggests that the colour changes in the phosphor involves an activation energy mechanism. This in itself also suggests that a measurement of the reflectance can be used to deduce the temperature, although not linearly.

4.0 Conclusion and Discussion

This article presents a simple method to determine the bandgap of a thermochromic phosphor. The phosphor is heated through its colour change temperature range while being illuminated by different wavelengths of light using discrete LEDs. A simple PD circuit allows the reflected light to be measured. Using the data obtained in the previous step, the absorbance as a function of wavelength can be calculated. To determine the phosphor's bandgap, we use the Schuster-Kubelka-Munk (SKM) function. We then place the material's color change in the context of phonons and activation energy, realizing that the reflectance versus temperature behavior appears to obey Arrhenius's law. Thermochromic phosphors are considered to be promising in photonic devices. They are actively being studied because of their apparent ability to tune the bandgap of many photoactive materials, especially for solar cell applications. This work is novel because it proposes a simple, plausible approach to determining bandgap, as well as an indication of the existence of an activation energy. There is considerable scope for future development, such as improving the wavelength range and resolution.

5.0 References

Ala-Laurila P., Donner K.& Koskelainen A. (2004). *Thermal activation and photoactivation of visual pigments, Biophysical Journal,* 86*, 3653–3662.*

Bos AS.J. (2017). Thermoluminescence as a Research Tool to Investigate Luminescence Mechanisms, *Materials,*10, 1357.

Byrd J.& Perona M. (2005). Kinetics of popping of popcorn. *Cereal Chemistry, Vol.*82(1), 53–59.

Davis E.A. & Mott N. (1971). Electronic processes in non-crystalline materials, Clarendon Press Oxford.

Day J.H.& Joachim A. (1965). Thermochromic Compounds II, *The Journal of Organic Chemistry,* 30, 4107–4111.

Dolgonos A., Mason T.O.& Poeppelmeier K.R. (2016). Direct optical band gap measurement in polycrystalline semiconductors: A critical look at the Tauc method, J*ournal of Solid-State Chemistry*, Vol. 240, 43–48.

Fu F.& Hu L. (2017). 15-temperature sensitive colour-changed composites, *Advanced High Strength Natural Fibre Composites in Construction,*ed Fan M. & Fu F. (Woodhead Publishing), 405 – 423, ISBN 978-0-08-100411-1

Hamam K.J.& Alomari M.I.,(2017). A study of the optical band gap of zinc phthalocyanine nanoparticles using UV–Vis spectroscopy and DFT function. *Applied Nanoscience,*Vol.7,261–268.

Hoffmann J., Lubbers D.& Heise H.(1998). Applicability of the Kubelka-Munk theory for the evaluation of reflectance spectra demonstrated for haemoglobin-free perfused heart tissue, *Physics in Medicine & Biology*, Vol. 43 (12), 3571-3587.

Kubelka P.(1948). New Contributions to the Optics of Intensely Light-Scattering Materials. Part I,J*. Opt. Soc. Am. Vol.*38, 1067-1067.

Kubelka P.(1954). New Contributions to the Optics of Intensely Light-Scattering Materials. Part II: Nonhomogeneous Layers, *J. Opt. Soc. Am., Vol.* 44, Issue 4, 330-335.

KortumG. (2012) Reflectance spectroscopy: principles, methods, applications, Springer Science &Business Media (2012)

Laidler K. J.(1972). Unconventional Applications of the Arrhenius Law,*Journal of Chemical Education, Vol.* 49, 343.

Li S.Y., Mlyuka N.R.,Primetzhofer D., Hallén A., Possnert G., Niklasson G.A. & Granqvist, C.G. (2013). Bandgap widening in thermochromic Mg-doped VO2 thin films: Quantitative data based on optical absorption, *Applied Physics Letters,* 103

Li, Y., Zhang, L., Torres-Pardo, A., González-Calbet,J. M., Ma, Y., Oleynikov, P., Terasaki O., Asahina S., Shima M., Cha D., et al. (2013). Cobalt phosphate-modified barium-doped tantalum nitride nanorod photoanode with 1.5% solar energy conversion efficiency. Nature Communications, 4(1), 3566.

Machado A. E., Gomes W. R., Araujo D., Miglio H. S., Ueno L.T., Paula R.D., Cavaleiro J. A.& Neto N. M.B.,(2011). *Molecules*,**16** 5807–5821.

Myrick M. L., Simcock M. N., Baranowski M.,BrookeH., Morgan S.L. & McCutcheon J.N.(2011). The Kubelka-Munk Formula Revisited, Applied Spectroscopy Reviews, Vol. 46,140-165.

Pankove J.I. (1975). Optical processes in semiconductors, *Courier Corporation*(1975). pin-spot2d Si photodiode. Last accessed: 20/04/2024 URL:https://za.rs-online.com/web/p/photodiodes/1837151/

RGB color codes. Last accessed 20/04/2024 URL: https://www.rapidtables.com/web/colour/RGB colour.html

Salom A., Zengin A., Candas A.& Bitlisli B.O. (2016). *Journal of Society of Leather Technologistsand Chemists*, 100, 314–320.

Schuster A, (1905). Radiation Through a Foggy Atmosphere, *The Astrophysical Journal,* 21, 1.

Singh P & Ravindra N (2010). *Journal of Materials Science*, 45, 4013–4020.

Soref R.& Bennett B. (1987). *IEEE Journal of Quantum Electronics*, 23, 123–129.

Tauc J. (1968). *Materials Research Bulletin,* 3, 37–46.

Weckhuysen B.M., Verberckmoes A.A., Debaere J., Ooms K, Langhans I.& Schoonheydt R. A., 2000.). *Journal of Molecular Catalysis A: Chemical,* 151, 115–131.

Wendlandt W.& Hecht H. (1969). *Reflectance Spectroscopy,*Wiley Intersciences, New York (1969).

Zanatta A.R., (2019). Revisiting the optical bandgap of semiconductors and the proposal of a unified methodology to its determination, Scientific Reports, 9, 1–12